Particle Accelerators, 1992, Vols. 37–38, pp. 519–530
Reprints available directly from the publisher
Photocopying permitted by license only

ANALYSIS OF HEAVY ION FUSION TARGETS

J. MEYER-TER-VEHN and M. MURAKAMI

Max-Planck-Institut für Quantenoptik, D-8046 Garching, FRG.

(Received 7 January 1990)

Indirectly driven targets for heavy ion fusion are discussed. In particular, results concerning the beam/x-ray conversion efficiency and target gain are given; $r^{1.5}R$ scaling is derived analytically.

1 INDIRECT DRIVE FOR HEAVY ION FUSION

For future progress in heavy ion fusion, it is indispensible to discuss the physics and the design of indirectly driven targets. Indirect drive may well be the superior option for imploding fusion capsules with heavy ion beams at the required level of spherical symmetry. Direct illumination of a capsule with not more than 1–2% rms asymmetry is already very difficult to achieve with lasers, but it is almost impractical with stiff heavy ion beams that deposit their energy deeply inside solid material. Since the concept of indirect drive is to convert the beam energy first into thermal x-rays in converter elements which are separated from the fusion capsule, the geometry of beam/target interaction and also the requirements on deposition power are quite different from direct drive. Details of target design therefore matter for both heavy ion driver development and relevant beam/target interaction experiments[1].

In this paper we start with a general discussion of different target designs in Section 2. A tutorial introduction to inertial confinement fusion (ICF) was given recently in Ref. 2, and for an overview on heavy ion fusion one may refer to Ref. 3. Still, there is no convincing answer in the published literature about the best heavy ion energy. The standard choice of 10-GeV Bi ions adopted in the HIBALL study[4] implies stopping ranges R = 0.1–0.3 g/cm^2. Accelerator designers tend to push for higher energies (50–100 GeV), whereas target design would greatly benefit from lower ion energies (1–2 GeV). Clearly, this is a most relevant question for the conceptual design of a test facility and an updated reactor scenario for heavy ion fusion. Not having a final answer, we give some arguments for the various options and thereby hope to stimulate the discussion.

The coupling efficiency of indirectly driven targets is then discussed in Section 3, and some basic formulas are given for orientation; an in-depth study on this topic is found in Ref. 5. Section 4 gives an analysis of converter elements[6] which are of stretched cylindrical shape, at least for higher ion energies. We present a simulation of a typical case, put much emphasis on the specific deposition power required for

high conversion efficiency, and give analytic results for the scaling of conversion efficiency. Section 5 deals with target gain.

2 DIFFERENT TARGET DESIGNS

For indirect drive, the beam is used to heat a small cavity (hohlraum) to temperatures of 200–300 eV. There are many ways to do this. A couple of options are sketched in Figure 1. Each target consists of an outer casing made of high-Z material, a fusion capsule indicated in Figures 1a–d by the dashed circle, and converter elements marked by the hatched areas. The space between these components is either vacuum forming the hohlraum or is filled with converter material as in Figure 1d. In this latter case the converter material must be of low density so that the dilute plasma filling the hohlraum during operation is of negligible hydrodynamic influence on the capsule and has an optical thickness ≈ 1 for its own thermal radiation; energy transport to the capsule has to occur by x-rays.

The option in Figure 1a is in a sense the most simple one. It has a single converter which is heated by a bundle of beams indicated by the arrows. Overlapping of several beams in the same deposition volume helps to achieve the required deposition power. The heated converter emits thermal x-rays which irradiate and heat the inner surface of the casing as well as part of the capsule. The essential point of radiation symmetrization in a hohlraum is that all surface areas heated by the primary x-rays will themselves start to radiate, and, as a consequence, the integrated radiation field becomes more and more isotropic by successive absorption and reemission steps. The reemission capability of different materials and the energy transfer between converter, outer wall, and capsule are discussed quantitatively in Ref. 5. The symmetry of x-ray deposition on the capsule is studied for different hohlraum geometries in Ref. 7. The problem with the one-sided illumination scheme in Figure 1a is that, at least for typical ICF parameters, the symmetrization is insufficient. The capsule receives considerably more radiation on the side facing the converter than on its rear side. Unless additional measures are taken, e.g., by screening or shimming the capsule, which however would degrade the overall efficiency, single converter designs do not give the required symmetry of 1–2% rms deviation[7].

A better option is shown in Figure 1b with two converter elements located at the poles of the stretched ellipsoidal casing. The symmetry analysis of this design shows that the quadrupole mode of the radiation field now represents the most dangerous asymmetry[7]. Screening of the capsule against direct irradiation from the hot poles by screening layers (black disks at the ends of the converter cylinders in Figure 1b) may be a method to reduce the quadrupole mode and to achieve the required symmetry. The size of the target is given by the fusion capsule which has a diameter of 5–10 mm for high-gain reactor-size targets; it is determined by the implosion and fusion physics. Since the surface area of the casing should not be larger than 10 times the capsule area (for reasons of transfer efficiency discussed below), the overall size of the target is 1–3 cm and the cylindrical converters may be 5–8 mm long. Consider-

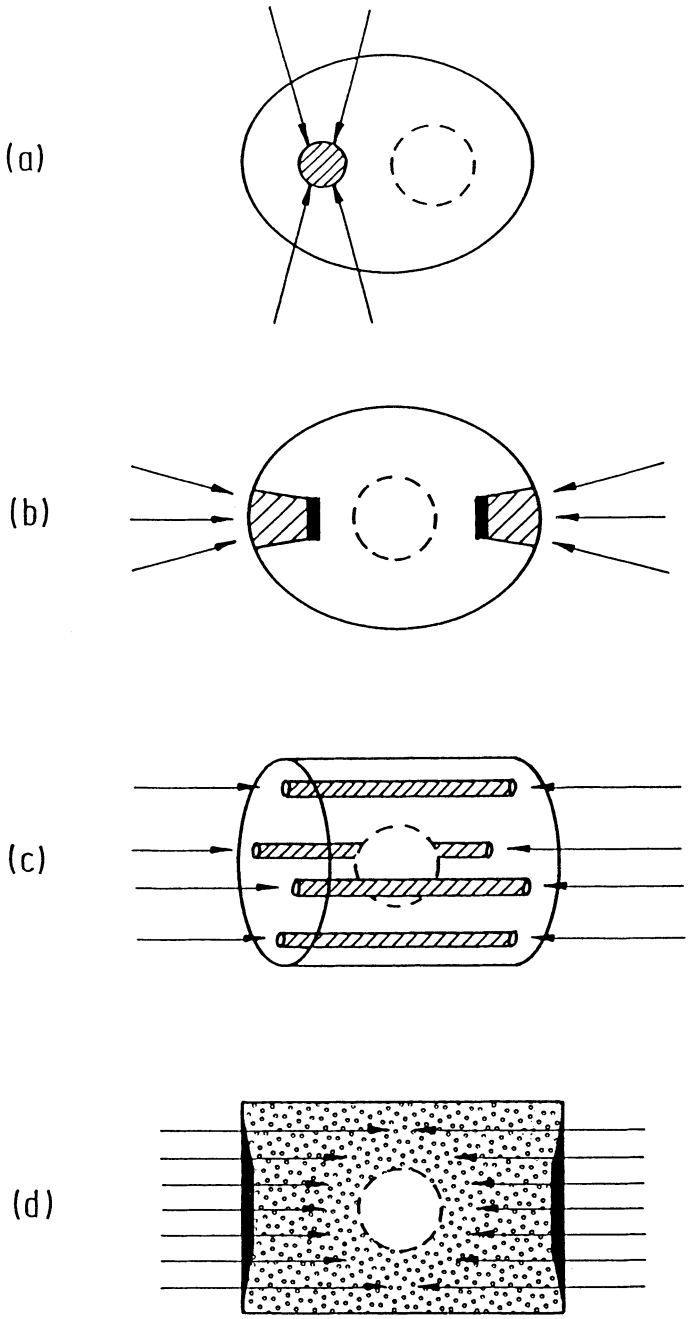

FIGURE 1 Different target configurations for indirectly driven heavy ion fusion. The arrows indicate ion beams, the hatched areas represent the converter elements, the solid lines mark the confining wall of the cavity, and the dashed circles give the location of the fusion capsule. In configuration (d) the cavity is filled with very low density converter material. For details see text.

ing foam converters with a density of about 0.5 g/cm^3, ion beams with ranges between 0.2–0.4 g/cm^2 can be stopped, adequate e.g. for 10-GeV Bi ions.

From the point of view of accelerator designers going to higher ion energies is favorable because then the required beam energy can be transported with less beam current and is easier to focus. It is therefore of interest to use the full size of the casing for beam stopping, possibly with a cage-like converter structure as shown in Figure 1c. The converter rods could be heated with beams from both sides to increase the deposition power. Their lengths should be matched with the stopping range in the heated material. The physics of heavy ion stopping in plasma including the atomic physics determining the effective charge are treated in Ref. 8. One could imagine stopping heavy ions up to 100 GeV. Having enhanced Bragg peak deposition at the end of the range, maximum x-ray emission is expected from the end regions of the rods producing good radiation symmetry. Of course, these targets have to be positioned and oriented very carefully with respect to the beam, and this may be a decisive disadvantage for an ICF reactor where targets have to be injected into the reactor chamber and shot by the beam at a rate of about 10 Hz.

From the point of view of target operation the scheme sketched in Figure 1d would be much more attractive. Here, the entire hohlraum is filled with converter material and the beam focus can be as large as the target cross-section. This design is rather insensitive against a small jitter of target position and orientation. In order to avoid that central parts of the ion beam hit the capsule, the front sides of the cylindrical casing should be shimmed appropriately. The problem with this type of target is that it is restricted to relatively low ion energies. This is because the total converter mass has to stay below 100 mg, as we will explain in Section 4; therefore the density of the converter material has to be small, about 10 mg/cm^2, and admissible stopping ranges will be 30 mg/cm^3, at most. This corresponds to heavy ions of 1–2 GeV. For light ion beam fusion, this type of target may be the only option, because light ion beams are difficult to focus.

3 TARGET MATERIALS AND TRANSFER EFFICIENCY

In this section, we briefly discuss the energetics of radiation transfer from the converter to the fusion capsule in a hohlraum target[5,9]. Each wall element facing the hohlraum and receiving radiation heats up and partially reemits the energy received. The physics of wall heating can be described in terms of ablative heat waves[10]; these waves have been observed recently in laser-heated cavities[11]. The flux $S_{in} = S_a + S_r$ incident on the wall splits up into the absorbed flux S_a and the reemitted flux S_r. We define the reemission factor as

$$N = S_r/S_a. \tag{3.1}$$

It is related to the albedo $S_r/S_{in} = N/(N+1)$. We have studied[5] the factor N by computer simulation for materials with different atomic number Z. The opacities were calculated based on the work of Eidmann and Tsakiris[12,13]. The overall result can be represented approximately in the form

$$N \approx 0.3 \cdot Z^{0.9} \cdot (t/10\ \text{ns})^{0.5}, \tag{3.2}$$

where a constant absorbed flux $S_a = 10^{14}$ W/cm^2 is assumed and t is the time. The factor N is found to depend on S_a only very weakly. On the other hand, it shows a pronounced dependence on Z. The reemission of gold ($Z = 79$) is 10 times larger than that of carbon ($Z = 6$). This allows to construct hohlraum targets with a reasonable transfer efficiency. Energy losses into the confining wall of the hohlraum are reduced by choosing high-Z material for the casing and low-Z material for the ablator of the fusion capsule. For the transfer efficiency which is the fraction of the converted x-ray power absorbed by the capsule, we find

$$\eta_{tra} = n/(a + n),$$

where

$$n = N_2/(N_1 + 1).$$

The reemission factor of the casing is N_2, and of the capsule, N_1. The variable a is given by the ratio

$$a = A_2/A_1$$

of the corresponding surface areas A_2 and A_1. In the derivation of this formula it is assumed that all primary x-rays from the converter first shine on the outer casing. Taking average values $N_1 \approx 1$ for carbon and $N_2 \approx 10$ for gold as estimates, one obtains a transfer efficiency

$$\eta_{\text{tra}} = 1/3$$

for an area ratio $a = 10$, characteristic for the configurations shown in Figure 1.

In addition to the transfer efficiency, the hydrodynamic efficiency η_{hyd} is important for the overall target coupling. It is defined as the final energy of the imploding fuel divided by energy absorbed by the capsule. It is well described by the spherical rocket model[14]. Assuming that 86% of the capsule mass is ablated, the hydrodynamic efficiency is

$$\eta_{\text{hyd}} = 18\text{–}20\%$$

for a carbon ablator, which is almost completely ionized for the ICF cavity temperatures of 200–300 eV. The rocket model also gives the implosion velocity

$$v_i \approx [3 \cdot 10^7 \text{ cm/s}][(T_1/200 \text{ eV})^{1/2}]$$

in terms of the temperature T_1 of the capsule's low-Z ablation plasma. Since the product $\eta_{\text{tra}} \cdot \eta_{\text{hyd}} \leq 10\%$ and the total coupling efficiency from beam to fuel should be at least 5% for a high-gain target, it is clear that the conversion efficiency of beam energy into thermal x-rays must be very high, in the range of 70–90%.

4 CONVERSION EFFICIENCY

4.1 Simulation of a Cylindrical Converter Element

The conversion configuration shown in Figure 2 was simulated with the one-dimensional radiation hydrodynamics code MULTI[15]. An ion beam is heating the

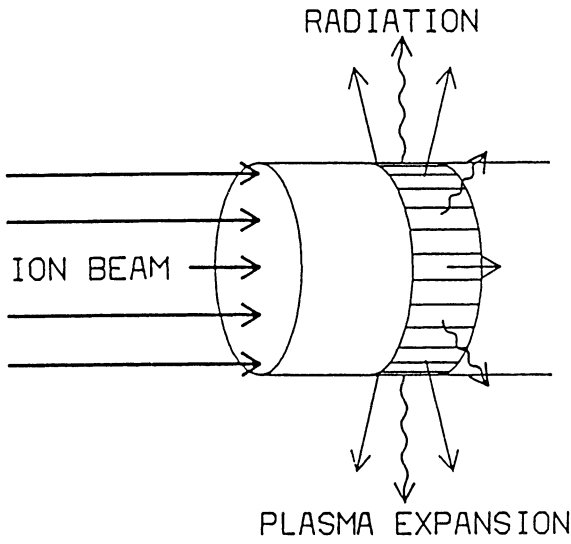

FIGURE 2 Schematic view of the cylindrical converter.

cylindrical converter uniformly with a specific deposition power of $3 \cdot 10^{16}$ W/g for 10 ns. The cylinder has a radius of 1.5 mm and is made of 0.3 g/cm^3 gold foam. The temperature evolution as a function of radius and time is plotted in Figure 3a. It is seen that the central temperature grows to 500 eV in about 1 ns and then stays almost constant over the working period of 9 ns. The spatial temperature profile drops to about 300 eV at the surface from where the thermal radiation is emitted. The radial optical thickness is about 10. The energy balance is given in Figure 3b. After the heating-up phase the absorbed energy is almost completely radiated, and the conversion into thermal x-rays reaches 90% finally. The kinetic energy plays a minor role; the cylinder expands to almost twice its original radius during the working ranges will be 30 mg/cm^3, at most. This corresponds to heavy ions of 1–2 GeV. For light ion beam fusion, this type of target may be the only option, because light ion beams are difficult to focus.

4.2 Specific Deposition Power Required for Heavy Ion Fusion

This shows that heavy ion beam energy can be converted into thermal x-rays with high efficiency, provided that sufficient specific power deposition

$$P = (1/\pi r^2) \cdot (dN_b/dt) \cdot (dE_{\text{ion}}/\rho dx) \tag{4.1}$$

is reached, which is directly related to the beam parameters, the focal area πr^2, the particle current dN_b/dt, and the stopping power $dE_{\text{ion}}/\rho dx$. In order to obtain 70–90% conversion efficiency required for indirect drive, specific deposition powers

$$P \geq 10^{16}\ W/g \tag{4.2}$$

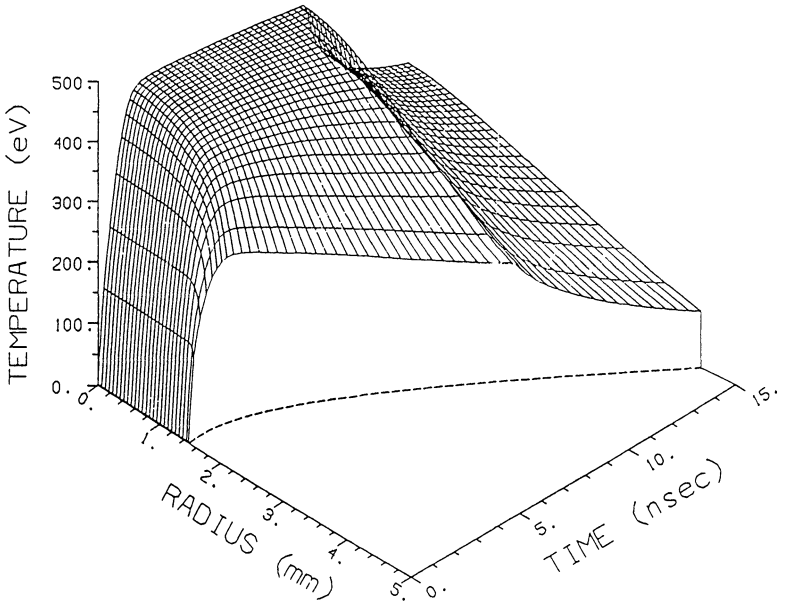

FIGURE 3a Temperature evolution as a function of radius and time of a cylindrical converter made of 0.3 g/cm^3 gold foam and driven by a deposition power of $3 \cdot 10^{16}$ W/g. For details see text.

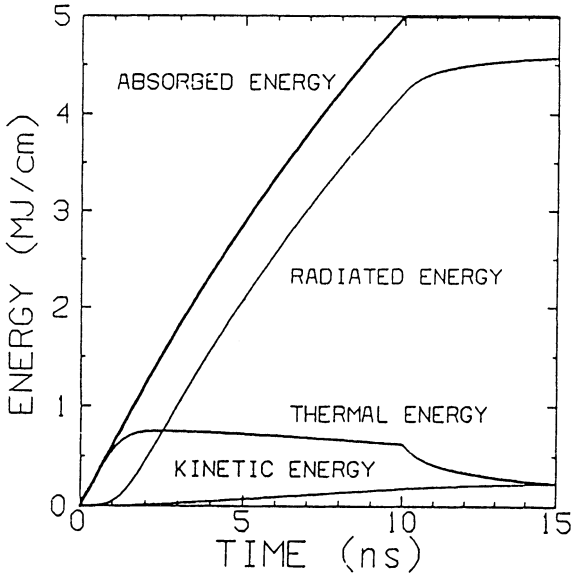

FIGURE 3b Energy flow diagram corresponding to the simulation shown in Figure 3a.

have to be achieved. This is about one order of magnitude more than the requirement for direct drive and represents an outstanding challenge for heavy ion beam fusion.

The physics setting these limits is remarkably simple. As we have observed in the simulation example given above, the internal energy E_h needed to heat the converter is the dominant loss factor. A simple, but useful estimate for the conversion efficiency is therefore

$$\eta_{\text{con}} \approx 1 - E_h/E_b. \tag{4.3}$$

The specific internal energy of gold and aluminum, as given by the SESAME equation-of-state (EOS) library[17], is plotted versus temperature for different densities in Figure 4. It is seen that the EOS is not strongly dependent on density. For gold, it can be represented by

$$e = 2.2 \cdot 10^{10}\,\text{erg/g} \cdot T(eV)^{1.6}, \tag{4.4}$$

and for aluminum by

$$e = 3.6 \cdot 10^{11}\,\text{erg/g} \cdot T(eV)^{1.2}. \tag{4.5}$$

These expressions hold at densities 0.1–1.0 g/cm^3, suitable for beam energy conversion. The required temperature is $T = 300$ eV or higher. It turns out that the temperature of 300 eV is only a lower limit. Depending on the optical thickness of the converter, larger temperatures are required (compare e.g. Figure 3a). From Figure 4 one finds the specific internal energy

$$e = 20\ \text{MJ/g} \tag{4.6}$$

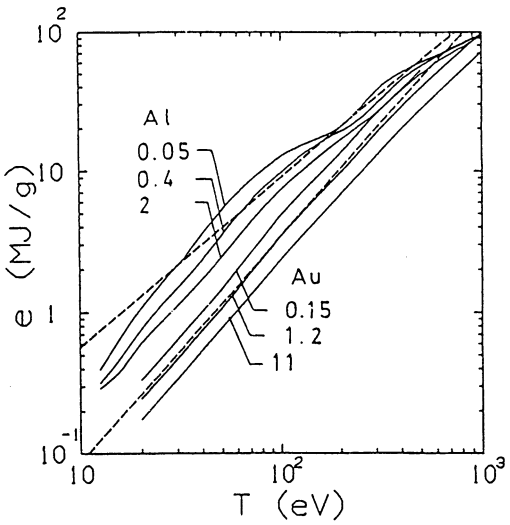

FIGURE 4 The specific internal energy versus temperature for gold and aluminum at different densities given as labels in units g/cm^3 The data are from the SESAME EOS Library[17]. The dashed lines represent the power law approximations given by Eqs. (4.4) and (4.5), respectively.

for 300 eV gold, and even more for aluminum and other low-Z materials at this temperature. This puts a severe limit on the usable converter mass. In order to keep the energy invested into converter heating below 1 MJ (or 20% of the 5-MJ driver energy needed to implode a reactor target), the converter mass should not exceed

$$M_{\text{con}} \leq 50 \text{ mg}. \tag{4.7}$$

Together with the required driving power of 500 TW, this leads to the lower bound (4.2) on the specific deposition power. The simple arguments given here are well confirmed by detailed simulations performed by different groups[6,16].

4.3 The $r^{1.5}R$ Scaling of Heavy Ion Targets

Given a certain target design, its linear dimensions scale with the driving beam energy E_b approximately like $\sim E_b^{1/3}$; also the ion stopping length L and the pulse time t_b, which is set equal to the implosion time, are scaled $\sim E_b^{1/3}$. On the other hand, it is assumed that the focal spot radius r of the beam and the ion range R which determine the converter mass,

$$M_{\text{con}} = \pi r^2 R, \tag{4.8}$$

may be varied independently of E_b, at least within the limits given by the target cross section. Since $R = \rho L$ and L is fixed by E_b, changing the ion energy E_{ion}, and thereby the ion range $R(E_{\text{ion}})$, is only possible by changing the converter density $\rho \sim R$. This is an important point in the following where a scaling formula of the conversion efficiency is derived.

Since the heating energy E_h is given by

$$E_h = e(T) \cdot M_{\text{con}}, \tag{4.9}$$

one might expect that the conversion efficiency (4.3) depends on r and R only through the mass and, therefore, through the combination r^2R. However, invariance with respect to $r^{1.5}R$ was observed in full-scale simulations of heavy ion fusion targets[18,19]. In fact, we show that this scaling behavior is obtained analytically when taking into account radiation diffusion in cylindrical converter elements. The simple power balance

$$E_b/t_b \approx \sigma T^4 F/\tau \tag{4.10}$$

leads to this result. Here, $F \approx 2\pi rL$ is the surface of the stretched cylindrical converter with length L, and

$$\tau = r/l_R \tag{4.11}$$

is its optical thickness in radial direction. The Rosseland mean free path l_R is taken in power-law approximation:

$$l_R \approx l_0 \cdot T^\alpha/\rho^\beta, \tag{4.12}$$

where l_0, α, and β are material constants. Solving Eq. (4.10) for T, one obtains

$$T \approx (E_b \cdot \rho^\beta/2\pi L t_b \sigma l_0)^{1/(4+\alpha)}. \tag{4.13}$$

The bulk temperature of the converter has to increase with density like $T \sim \rho^{\beta/(4+\alpha)}$. Using $\rho = R/L$ and $e(T) = e_0 \cdot T^{\mu}$, we find

$$\eta_{\text{con}} = 1 - e(T) \cdot M_{\text{con}}/E_b = 1 - F_0 \cdot r^2 \cdot R^{1+\mu\beta/(4+\alpha)}/E_b, \tag{4.14}$$

with

$$F_0 = \pi e_0 (E_b/2\pi L^{1+\beta} t_b \sigma l_0)^{\mu/(4+\alpha)}. \tag{4.15}$$

The parameters α, β, and μ, as well as the characteristic combinations of these parameters, are given for plastic, aluminum, and gold in Table 1. First, it is noticed that $\mu\beta/(4+\alpha) \approx 0.3$ for all materials, which means that $(1 - \eta_{\text{con}}) \sim r^2 R^{1.3} \sim (r^{1.54} R)^{1.3}$. This explains the $r^{1.5}R$ scaling found in simulations[18,19]; apparently, it is more naturally expressed in the form $r^2 R^{1.3}$. Secondly, the combination $\mu(1-\beta)/3(4+\alpha)$, which is the exponent of E_b in the expression (4.15) for F_0 taking into account that L and $t_b \sim E_b^{1/3}$, is close to zero for all materials so that F_0 is approximately independent of E_b. Adjusting F_0 to the results of the conversion model of Ref. 6, we obtain the approximate formula

$$\eta_{\text{con}} \approx 1 - 350 \cdot r\,(\text{cm})^2 R\,(\text{g/cm}^2)^{1.3}/E_b(MJ), \tag{4.16}$$

which holds for two converter elements. In case that N_C converters are considered, the factor 350 in Eq. (4.16) has to be multiplied by $(N_c/2)^{1-\mu/(4+\alpha)}$. Essentially the same results for η_{con} were derived independently by S. Atzeni[20].

5 GAIN OF HEAVY ION TARGETS

The target gain is the released fusion energy divided by the beam energy invested to drive the target to ignition. It depends in a complicated way on the beam parameters and the target design, and sophisticated numerical simulation is required to predict the gain. However, the results of such simulations have been modeled rather successfully by simple analytic means, assuming that the imploded fuel at the point of stagnation is isobaric and consists of a hot igniting region in the centre surrounded by highly compressed, cold fuel. The model is described in detail in Ref. 21. The model gain depends on three parameters:

1) the coupling efficiency $\eta_C = E_{\text{fuel}}/E_b$, describing the fraction of beam energy transferred to the fuel at ignition;

TABLE 1
Equation-of-State and Opacity Parameters for Different Materials

	Plastic	Aluminum	Gold
μ	1.2	1.2	1.6
α	4.0	2.5	1.0
β	2.0	1.5	1.0
$\mu\beta/(4+\alpha)$	0.30	0.28	0.32
$\mu(1-\beta)/(12+3\alpha)$	0.05	0.03	0.00

2) the pressure p of the isobaric fuel, related to the radius R_S of the hot central region by $R_S = 15\ \mu\text{m}/p$ (Tbar); and

3) the isentrope parameter $\alpha_p = p/p_{\text{deg}}$, describing the entropy of the highly compressed fuel (p_{deg} is the degenerate electron pressure for $T = 0$ fuel).

For the gain of indirect drive heavy ion beam fusion, the coupling efficiency is represented by

$$\eta_c = \eta_{\text{con}} \cdot \eta_{\text{tra}} \cdot \eta_{\text{hyd}},$$

where η_{tra} is the transfer efficiency of x-rays from the converter to the pellet and η_{hyd} the hydrodynamic efficiency of pellet implosion. Taking $\eta_{\text{tra}} = 0.35$, $\eta_{\text{hyd}} = 0.20$, $p = 0.2$ Tbar, $\alpha = 3.5$ and η_{con} according to Eq. (4.16), we have calculated gain curves and have plotted them as solid lines in Figure 5. For comparison, also the Livermore gain predictions for heavy ion beam fusion[18] based on detailed simulation, are given as dashed lines, and close agreement is found. The dotted curve in Figure 5 corresponds to $\eta_{\text{con}} = 100\%$. This "ideal" gain curve is degraded by incomplete x-ray conversion. The realistic curves are labeled by the $r^{3/2}R$ parameter which is easily transferred into the $r^2R^{1.3}$ product needed in Eq. (4.16). A more extended presentation of these model results for the gain of heavy ion fusion targets will be given in a separate paper[22].

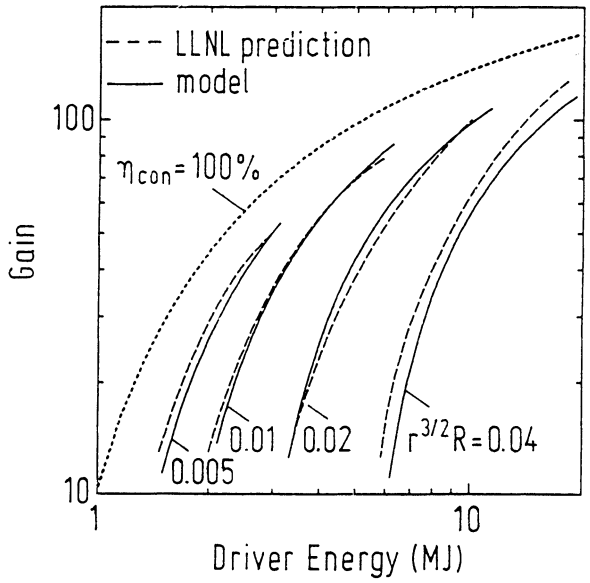

FIGURE 5 Gain curves for indirectly driven heavy ion fusion targets as a function of driver energy. The solid curves are model results corresponding to $p = 0.2$ Tbar, $\alpha = 3.5$, $\eta_{\text{tra}} \cdot \eta_{\text{hyd}} = 0.07$, and different values of $r^{3/2} \cdot R$ with radius r in cm and range R in g/cm^2. The dashed curves are Livermore gain predictions[18] obtained from detailed numerical simulations. The dotted curve corresponds to an ideal converter with 100% efficiency.

ACKNOWLEDGEMENTS

The authors acknowledge intensive discussions with S. Atzeni, M. Basko, and R. Ramis on the topic of this paper. The work was supported in part by the Bundesministerium für Forschung und Technologie and by Euratom.

REFERENCES

1. J. Meyer-ter-Vehn, S. Witkowski, R. Bock, D. H. H. Hoffmann, I. Hofmann, R. W. Müller, R. Arnold and P. Mulser, *Phys. Fluids B* **2**, 1313 (1990).
2. J. Meyer-ter-Vehn, in Proceedings of the International School of Physics "Enrico Fermi", Course CXVI, Varenna (Italy), 10–20 July 1990, edited by E. Sindoni, to be published (1991).
3. J. Meyer-ter-Vehn, *Plasma Phys. Controlled Fusion* **31**, 1613 (1989).
4. D. Böhne, I. Hofmann, G. Kessler, G. L. Kulcinski, J. Meyer-ter-Vehn, U. von Möllendorff, G. A. Moses, R. W. Müller, I. N. Sviatoslavky, D. K. Sze and W. Vogelsang, *Nuclear Engineering and Design* **73**, 195 (1982).
5. M. Murakami and J. Meyer-ter-Vehn, *Nuclear Fusion* **31**, 1315 (1991).
6. M. Murakami, J. Meyer-ter-Vehn, and R. Ramis, *J. X-Ray Sci. Tech.* **2**, 127 (1990).
7. M. Murakami and J. Meyer-ter-Vehn, *Nuclear Fusion* **31**, 1333 (1991).
8. Th. Peter and J. Meyer-ter-Vehn, *Phys. Rev. A* **43**, 1998 and 2015 (1991).
9. A. Caruso, in Inertial Confinement Fusion, Proceedings of the International School of Plasma Physics. "Piero Caldirola", Varenna, Italy, Sept. 1988, edited by A. Caruso and E. Sindoni (Editrice Compositori, Bologna, 1988), p. 139.
10. R. Pakula and R. Sigel, *Phys. Fluids* **28**, 232 (1985).
11. R. Sigel, G. D. Tsakiris, F. Lavarenne, J. Massen, R. Fedosejevs, J. Meyer-ter-Vehn, M. Murakami, K. Eidmann, S. Witkowski, H. Nishimura, Y. Kato, H. Takabe, T. Endo, K. Kondo, H. Shiraga, S. Sakabe, T. Jitsuno, M. Takagi, C. Yamanaka, and S. Nakai, *Phys. Rev. Lett.* **65**, 587 (1990).
12. G. D. Tsakiris and K. Eidmann, *J. Quant. Spectrosc. Radiat. Transfer* **38**, 353 (1987).
13 K. Eidmann, in Inertial Confinement Fusion, Proceedings of the International School of Plasma Physics. "Piero Caldirola", Varenna, Italy, Sept. 1988, edited by A. Caruso and E. Sindoni, Editrice Compositori, Bologna, 1988, p. 65.
14. M. Murakami and K. Nishihara, *Jpn. J. Appl. Phys.* **26**, 1132 (1987).
15. R. Ramis, R. Schmalz, J. Meyer-ter-Vehn, *Comp. Phys. Comm.* **49**, 475 (1988).
16. J. D. Lindl, R. O. Bangerter, J. Mark and Yu-LiPan, in "Heavy Ion Fusion," edited by M. Reiser, T. Godlove, and R. Bangerter, AIP Conference Proceedings (American Institute of Physics, New York, 1986), p. 89.
17. B. I. Bennett, J. D. Johnson, G. I. Kerley, and G. T. Rood, Los Alamos National Laboratory Report LA-7130 (1978).
18. R. O. Bangerter, J. W. Mark, and A. R. Thiessen, *Phys. Lett. A* **88**, 225 (1982).
19. J. D. Lindl, R. O. Bangerter, J. W. Mark, and Yu-LiPan, *Fusion Technol.* **13**, 348 (1988).
20. S. Atzeni, contribution "2-D study of thermal x-ray generation from ion beam heated converters," these *Proceedings*.
21. J. Meyer-ter-Vehn, *Nuclear Fusion* **22**, 561 (1982).
22. S. Atzeni, J. Meyer-ver-Vehn, and M. Murakami, to be published (1991).